ANNALS of Clinical and Translational Neurology
Open Access
ANA American Neurological Association since 1875

RESEARCH ARTICLE

Periventricular white matter changes in idiopathic intracranial hypertension

Alessia Sarica[1,*], Maria Curcio[2,*], Laura Rapisarda[2], Antonio Cerasa[3,4], Aldo Quattrone[1,3] & Francesco Bono[2]

[1]Department of Medical and Surgical Sciences, Neuroscience Centre, Magna Græcia University of Catanzaro, Catanzaro, Italy
[2]Department of Medical and Surgical Sciences, Center for Headache and Intracranial Pressure Disorders, Institute of Neurology, Magna Græcia University of Catanzaro, Catanzaro, Italy
[3]Neuroimaging Research Unit, Institute of Bioimaging and Molecular Physiology, National Research Council, Catanzaro, Italy
[4]S. Anna Institute and Research in Advanced Neurorehabilitation, Crotone, Italy

Correspondence
Francesco Bono, Center for Headache and Intracranial Pressure Disorders, Institute of Neurology, Department of Medical and Surgical Sciences, Magna Græcia University of Catanzaro, University Campus "S. Venuta", viale Europa, 88100 Catanzaro, Italy. Tel: +3909613647269; Fax: +3909613647177; E-mail: f.bono@unicz.it

Funding Information
No funding information provided.

Received: 29 June 2018; Revised: 25 September 2018; Accepted: 5 October 2018

Annals of Clinical and Translational Neurology **2019; 6(2): 233–242**

doi: 10.1002/acn3.685

*These authors contributed equally to the manuscript.

Abstract

Objective: To evaluate whether increased cerebrospinal fluid (CSF) pressure causes alteration of periventricular white matter (WM) microstructure in patients with idiopathic intracranial hypertension (IIH). **Methods**: In a prospective study, patients with refractory chronic headache with and without IIH performed a neuroimaging study including 3T MRI, 3D Phase Contrast MR venography, and diffusion tensor imaging (DTI) of the brain. Whole-brain voxel-wise comparisons of DTI abnormalities of WM were performed using tract-based spatial statistics. A correlation analysis between DTI indices and CSF opening pressure, highest peak, and mean pressure was also performed in patients with IIH. **Results**: We enrolled 62 consecutive patients with refractory chronic headaches. Thirty-five patients with IIH, and 27 patients without increased intracranial pressure. DTI analysis revealed no fractional anisotropy changes, but decreased mean, axial, and radial diffusivity in body (IIH_{MD} = 0.80 ± 0.04, non-IIH_{MD} = 0.84 ± 0.4, IIH_{AD} = 1.67 ± 0.07, non-IIH_{AD} = 1.74 ± 0.05, IIH_{RD} = 0.38 ± 0.04, non-IIH_{RD} = 0.42 ± 0.05 [$mm^2/sec \times 10^{-3}$]) of corpus callosum, and in right superior corona radiata (IIH_{MD} = 0.75 ± 0.04, non-IIH_{MD} = 0.79 ± 0.05, IIH_{AD} = 1.19 ± 0.07, non-IIH_{AD} = 1.28 ± 0.09, IIH_{RD} = 0.59 ± 0.03, non-IIH_{RD} = 0.53 ± 0.03 [$mm^2/sec \times 10^{-3}$]) of 35 patients with IIH compared with 27 patients without increased intracranial pressure. DTI indices were negatively correlated with high CSF pressures ($P < 0.05$). After medical treatment, eight patients showed incremented MD in anterior corona radiata left and right and superior corona radiata right. **Conclusions**: There is significant DTI alteration in periventricular WM microstructure of patients with IIH suggesting tissue compaction correlated with high CSF pressure. This periventricular WM change may be partially reversible after medical treatment.

Introduction

The syndrome of idiopathic intracranial hypertension (IIH) is a condition of increased cerebrospinal fluid (CSF) pressure without identifiable cause, which may occur with and without papilledema.[1–6]

Typical intracranial and periorbital MRI findings in patients with IIH include empty sella turcica,[7] flattening of the posterior aspect of the globe, optic nerve protrusion, and distension of the perioptic subarachnoid space.[8,9] Moreover, sinovenous stenosis is more common in patients with IIH than in subjects with normal CSF pressure.[10,11]

Although the presence of hyperintensities in T2 MRI revealed periventricular white matter (WM) macrostructure alteration in patients with intracranial hypertension associated with hydrocephalus,[12] similar finding in patients with a less severe intracranial pressure disorder

such as IIH were not found.[5–10] However, continuous CSF pressure recordings revealed the presence of abnormal pressure pulsations in patients with IIH too.[13] Whether these abnormal CSF pressure pulsations cause a permanent or reversible periventricular WM microstructure damage in patients with IIH is unknown.

It is now recognized that Diffusion Tensor Imaging (DTI), a non-invasive method based on the diffusion characteristics of water which recognizes the random motion of water molecules and where it is restricted by biological barriers,[14] is one of the most sensitive and promising MRI-based diagnostic tools for detecting subtle microstructural cerebral WM changes.[15,16]

Since we hypothesize that abnormal CSF pressure pulsations associated with increased intracranial pressure producing a mechanical compression against the wall of the lateral ventricles cause a tissue compaction leading to change in axonal organization in periventricular WM tissue microstructure of patients with IIH, we consider DTI method as suitable for investigating this issue.

Indeed, the presence of permanent or reversible DTI alterations in WM tissue microstructure could be relevant to patients with IIH for evaluating disease progression or resolution and to assess the efficacy of treatment. To address our hypothesis, we compared the periventricular WM tissue microstructure integrity in patients with refractory chronic headache with and without IIH by using DTI analysis. Additionally, we compared eight patients with IIH, who had follow-up clinical evaluation, CSF pressure monitoring, and DTI measurement with their baseline.

Methods

Institutional Review Board approval was obtained for the study, and written informed consent was obtained from all of the participants.

In this prospective study patients with IIH and patients with refractory chronic headache[17] without increased intracranial pressure, considered as our control group, were consecutively screened among the patients admitted to the Center for headache and intracranial pressure disorders of the Institute of Neurology in Catanzaro. Inclusion criteria in this study were refractory chronic headache with and without IIH, normal gadolinium enhanced MR of the brain, no history of systemic disease and cerebral venous thrombosis, or drug intake known to be associated with high CSF pressure. The criteria for exclusion from this study were abnormal neurological examination (except for papilloedema and sixth nerve palsy), hydrocephalus or cerebral venous thrombosis, MR evidence of structural brain lesions.

Assessment

We gave participants the same standardized forms to obtain headache, general medical (including body mass index: weight in kilograms divided by the square of height in meters), neurological, ophthalmological, and family histories. Chronic migraine (CM), chronic tension-type headache (CTTH), and idiopathic intracranial hypertension were diagnosed according to ICHD-3[17] and updated criteria for IIH.[1,17] In particular, enrolled patients with IIH has been diagnosed with CSF pressure >250 mm, measured by lumbar puncture monitoring, and they showed headache that developed in temporal relation to IIH, relieved by reducing intracranial hypertension and aggravated in temporal relation to increase in intracranial pressure. The headache was accompanied by either or both of the following: pulsatile tinnitus, papilloedema.

Neurological and ophtalmological examinations were conducted on patients by the same neurologists and ophtalmologists. The participants performed both brain magnetic resonance (MRI) and cerebral MR venography (MRV) before lumbar puncture (LP), with a time gap of 24/48 h. Moreover, all patients suspected of having elevated CSF pressure underwent LP in order to measure CSF opening pressure and to monitor CSF pressure for one-hour through a spinal puncture needle.

Furthermore, during the follow-up treated patients with IIH were evaluated at 3 months and they underwent a brain MRI within 3–6 months from the baseline.

CSF pressure measurement

The same operator (FB) performed LP and 1-hour lumbar CSF pressure monitoring through a spinal puncture needle by using a technique described elsewhere.[13] In brief, in a puncture room with the subject in the left lateral decubitus position a standard 22-gauge spinal needle (only occasionally 20 gauge) with three-way stopcock was inserted. A pressure cable linked the transducer to the monitor (Passport V, Datascope Corporation, Mahwah, NJ, USA). The pressure transducer (Transducer kit, Edwards Lifesciences, Irvine, CA, USA) was attached to the hub of the needle by using a 10 cm long flexible tube, it was then zeroed. CSF opening pressure was recorded for 4 minutes. Immediately after, CSF pressure was also monitored for a 1-hour period to analyze the mean pressure, peak and highest pulse amplitude, and abnormal pressure waveforms.

MRI data acquisition

Data were acquired on a 3T unit with an 8-channel head coil (Discovery MR-750, General Electric, Milwaukee, WI,

USA). Our routine protocols, published elsewhere,[18,19] included: (1) 3D T1-weighted spoiled gradient echo (SPGR) sequence (TE/TR = 3.7/9.2 msec, flip angle 12°, voxel- size $1 \times 1 \times 1$ mm^3; 368 sagittal slices), T2-weighted fast spin echo and T2-weighted FLAIR sequences; (2) 3D MR venography of the brain oriented in the sagittal plane[18] (Sag Inhance 3D Velocity, TE/TR = 5/10 msec, matrix size 384×384; slice thickness 1.4 mm); (3) diffusion-weighted acquisition[19] using spin-echo echo-planar imaging (TE/TR = 87/10,000 msec; bandwidth 250KHz; matrix size 128×128; 80 axial slices, voxel size $2.0 \times 2.0 \times 2.0$ mm^3) with 27 isotropically distributed orientations for the diffusion-sensitizing gradients at a *b*-value of 1.000 sec/mm^2. Head movements were minimized using foam pads around the participants' head.

DTI analysis

Diffusion-weighted images were processed using the tools of FMRIB (FSL 5.0, www.fmrib.ox.ac.uk). DTI scans were first corrected for distortion induced by eddy currents and head motions using the Diffusion Toolbox[20] (FDT). A diffusion tensor model was then fitted at each voxel, generating fractional anisotropy (FA), mean diffusivity (MD), axial diffusivity (AD), and radial diffusivity (RD) maps. A tract-based spatial statistics (TBSS) analysis was applied for exploring abnormalities of WM structures. Briefly, TBSS first nonlinearly registered subjects' FA images to the FMRIB58_FA atlas provided within FSL. In a second step, the mean FA images were projected onto an alignment invariant tract representation, the "skeleton", which was thresholded at an FA > 0.2[20] to include only WM voxels. This process of projecting individual maps onto a mean skeleton was also applied on MD, AD, and RD images. Differences in diffusion metrics between groups were assessed with a permutation-based inference for nonparametric statistical thresholding (tool "randomize" of FSL with 5000 permutations) and a two-samples unpaired *t*-test adjusted for age, gender, and disease duration. The resulting statistical maps were thresholded at $P < 0.05$ using threshold-free cluster enhancement (TFCE) with the family wise error (FWE) correction for multiple comparison.[20] The follow-up TBSS evaluated whether these patients showed changes in DTI indices after the medical treatment.

Statistical analysis

Statistical analysis was performed using the Statistical Package for Social Science software (SPSS, v20.0, Chicago, IL, USA) for Macintosh. For continuous variables, means of patient groups were compared using the two-samples unpaired *t*-test or Mann–Whitney test, as appropriate. For categorical variables, counts and percentages are reported. Differences in frequency distributions between groups were assessed using the Chi-squared test or Fisher's exact test, as appropriate. A statistically significant result was considered if $P < 0.05$ and when not explicitly specified, all *P* values were two-tailed.

The regions in which there were significant DTI differences between groups, were extracted with automatic atlas (JHU ICBM-DTI-81 White-Matter Labels) queries and averaged for two further analyses: (1) intragroup comparisons taking into account the CM and CTTH profiles, separately in patients with IIH and patients without IIH, and an intergroup analysis for comparing patients without IIH with CM and patients with IIH with CM; (2) linear regression against CSF pressure measures, where subjects' mean diffusion values were the dependent variable and each of the three pressures the independents. Post-hoc comparisons were made using two-samples unpaired *t*-test corrected according to the Bonferroni's method ($P < 0.05/11 = 0.0045$). For the longitudinal analysis of a small group of treated patients with IIH, a paired *t*-test was used by applying multiple correction as described as above.

Results

The characteristics of the 62 participants are summarized in Table 1. Bilateral transverse sinus stenosis on cerebral MRV was found in the majority (77%) of patients with IIH (Table 1). All participants had no evidence of periventricular white matter hyperintensities on T2 FLAIR of brain MRI. Of the initial cohort 47 patients suspected of having IIH underwent LP and one-hour lumbar CSF pressure monitoring. The remaining 15 patients with primary headache disorder, were not suspected of having high CSF pressure and did not undergo LP puncture. CSF pressure findings are shown in Table 2. According to CSF measurement findings the 47 patients were divided into two groups. The Group 1, including patients with IIH, showed elevated CSF opening pressure (mean 310 mmH_2O; SD 52), mean CSF pressure (mean 320 mmH_2O; SD 45) and highest peak pressure (mean 420 mmH_2O; SD 50), associated with abnormal pressure waves. The Group 2, including 12 patients without IIH, had normal opening pressure (mean 166 mmH_2O, SD 18) and normal mean CSF pressure (mean 167 mmH_2O, SD 19) with normal highest peak pressure (mean 205 mmH_2O, SD 25).

During the follow-up, only eight treated patients with IIH accepted to undergo a brain MRI acquisition and lumbar CSF pressure monitoring. Clinical evaluation and CSF pressure monitoring at 3 months revealed an improvement of headache rating scales and a normalization of CSF pressure values in these patients (Table 4).

Table 1. Demographics and clinical characteristics of 62 headache sufferers divided into 35 patients with IIH and 27 patients without increased intracranial pressure.

	Patients with IIH (n = 35)	Patients without IIH (n = 27)	P-value
Age, years, mean ± SD	40.71 ± 13.20	39.44 ± 10.61	0.676[1]
Disease duration, years, mean ± SD	2.48 ± 2.12	12.81 ± 11.18	<0.001[2]
Body mass index, kg/m^2, mean ± SD	32.84 ± 4.34	24.39 ± 4.75	<0.001[2]
Gender, F/M	31/4	22/5	0.48[3]
Headache diagnosis, *n* (%)			
Chronic Migraine	25 (71)	17 (63)	0.48[3]
Chronic Tension – Type headache	9 (26)	6 (22)	0.75[3]
Other	1 (3)	4 (15)	0.16[3]
Headache profile, *n* (%)			
Unilateral	18 (51)	18 (67)	0.23[3]
Bilateral	17 (49)	9 (33)	0.23[3]
Pulsating pain	18 (51)	18 (67)	0.23[3]
Severe	25 (71)	22 (81)	0.36[3]
Daily	35 (100)	27 (100)	NA
Nausea/vomiting	14 (40)	16 (59)	0.13[3]
Photo/phonophobia	17 (48)	20 (74)	0.04[3]
Aggravated with coughing	22 (63)	8 (30)	0.01[3]
Positional headache	28 (80)	0	NA
Nocturnal head pain attacks	24 (69)	0	NA
Associated Symptoms and signs, *n* (%)			
Visual disturbances	31 (89)	0	NA
Pulsatile Tinnitus	20 (57)	0	NA
Intracranial noise	5 (14)	0	NA
Vertigo	17 (49)	0	NA
Papilloedema	29 (83)	0	NA
Sixth nerve palsy	19 (54)	0	NA
Neuroimaging findings, *n* (%)			
Empty sella turcica	26 (74)	0	NA
Distention of the perioptic subarachnoid space with and without a tortuous optic nerve	30 (86)	0	NA
Optic nerve protrusion	28 (80)	0	NA
Bilateral TSS	27 (77)	0	NA

Data are given as mean ± SD.
NA, Not applicable; TSS, transverse sinus stenosis.
[1]Two-samples unpaired *t*-test.
[2]Mann–Whitney test.
[3]Chi-Square or Fisher's exact test.

TBSS voxel-wise data analysis

Compared with patients without IIH, patients with IIH showed no difference in FA, while they had significantly lower MD, AD, and RD as reported in Table 3. Patients with IIH had lower MD in WM.

Regions of body, genu, and splenium of the corpus callosum (CC); bilateral superior corona radiata (SCR); and right anterior corona radiata (ACR) (Fig 1A). Lower AD values appeared in the body and splenium of CC and in right SCR (Fig 1B). Patients with IIH showed also lower RD in the body of CC and right SCR (Fig 1C).

Figure 1D reported in green the overlap of the lower values of MD, AD, and RD of the IIH group, in the body of CC and in the right SCR. The overlap of lower MD and AD, without changes in other indices, is shown in blue in the splenium of CC. The overlapping regions with lower AD and lower RD were sparse voxels in the body of CC and resulted to be the same clusters of the overlapping of lower MD and lower RD (in yellow), which presented other few voxels in the right SCR.

The post hoc analysis revealed that no differences survived at Bonferroni correction when the means of the 11 abnormal regions were compared between: (1.a) patients

Table 2. Cerebrospinal fluid pressure findings in 47 headache sufferers who underwent lumbar puncture and one-hour lumbar CSF pressure monitoring through spinal puncture needle.

	Group 1 Elevated CSF pressure (n = 35)	Group 2 Normal CSF pressure (n = 12)	*P*-value
CSF pressure, mmH_2O, mean ± SD			
Opening pressure	310 ± 52	166 ± 18	<0.001[1]
Mean pressure	320 ± 45	167 ± 19	<0.001[1]
Highest peak pressure	420 ± 50	205 ± 25	<0.001[1]
Abnormal pressure waves, *n* (%)	35 (100)	0	NA

Data are given as mean ± SD.
CSF, cerebrospinal fluid; NA, Not applicable.
[1]Two-samples unpaired t-test.

without IIH with CM and patients without IIH with CTTH; (1.b) patients with IIH with CM and patients with IIH with CTTH. On the contrary, patients with IIH with CM had lower AD than patients without IIH with CM in the body and splenium of corpus callosum and in the right superior corona radiata (differences surviving at Bonferroni correction, $P < 0.0045$).

Regression analysis demonstrated that there were significant ($P < 0.05$) negative correlations among the average AD values and all the three CSF pressures, as showed in Figure 2A. In particular, significant results were found between body of CC and CSF opening pressure ($r = -0.402$, $P = 0.042$), highest peak pressure ($r = -0.386$, $P = 0.022$) and CSF mean ($r = -0.364$, $P = 0.023$), between splenium of CC and CSF opening pressure ($r = -0.419$, $P = 0.034$), highest peak pressure ($r = -0.405$, $P = 0.029$) and CSF mean ($r = -0.418$, $P = 0.024$), and between right SCR and CSF opening ($r = -0.436$, $P = 0.025$), highest peak pressure ($r = -0.344$, $P = 0.04$) and CSF mean pressure ($r = -0.394$, $P = 0.018$). Figure 2B reported one-hour lumbar CSF pressure monitoring through spinal needle of one patients with normal CSF pressure (on the left) and of one patient with elevate CSF pressure (IIH, on the right). The longitudinal analysis of eight patients with IIH revealed a significant increase in MD at the follow-up bilaterally in the anterior corona radiata and in the right superior corona radiata, while no changes in FA, AD or RD were found. Mean MD values, survived at the Bonferroni correction for the paired *t*-test, are reported in Table 4. All of the treated patients with IIH showed at the follow-up a regression of signs and symptoms when the CSF pressure normalized (Table 4).

Discussion

The diffusion tract-based analysis demonstrates a morphological variation in the periventricular WM microstructure in patients with IIH compared to patients with refractory chronic headache without increased intracranial pressure. For the first time, this DTI study highlights a subtle microstructural in vivo change in periventricular WM of patients with IIH. These periventricular WM microstructural changes observed in patients with IIH were partially reversible when CSF pressure normalized after medical treatment, suggesting that DTI may be used for evaluating disease resolution and to assess the efficacy of treatment.

These DTI alterations of periventricular WM microstructure in patients with IIH consisted of lower values of mean, axial and radial diffusivity without any

Table 3. Diffusion tensor imaging metrics of white matter regions significantly different between patients with and without increased intracranial pressure.

WM regions	Side	Metric	Patients with IIH (n = 35)	Patients without IIH (n = 27)	*P*-value
Body of CC		MD	0.80 ± 0.04	0.84 ± 0.04	<0.001[1]
		AD	1.67 ± 0.07	1.74 ± 0.05	<0.001[1]
		RD	0.38 ± 0.04	0.42 ± 0.05	0.001[1]
Genu of CC		MD	0.80 ± 0.04	0.84 ± 0.04	<0.001[1]
Splenium of CC		MD	0.74 ± 0.05	0.77 ± 0.04	0.003[1]
		AD	1.70 ± 0.06	1.78 ± 0.06	<0.001[1]
Anterior corona radiata	Right	MD	0.75 ± 0.04	0.79 ± 0.04	0.007
Superior corona radiata	Right	MD	0.75 ± 0.04	0.79 ± 0.05	0.003[1]
		AD	1.19 ± 0.07	1.28 ± 0.09	<0.001[1]
		RD	0.59 ± 0.03	0.53 ± 0.03	<0.001[1]
	Left	MD	0.74 ± 0.05	0.77 ± 0.03	0.005

Data are given as mean ± SD.
WM, white matter; IIH, idiopathic intracranial hypertension; CC, Corpus callosum; MD, mean diffusivity; AD, axial diffusivity; RD, radial diffusivity.
[1]Significant at Bonferroni correction $P < 0.0045$. Average MD, AD, and RD are expressed in units of $mm^2/s \times 10^{-3}$.

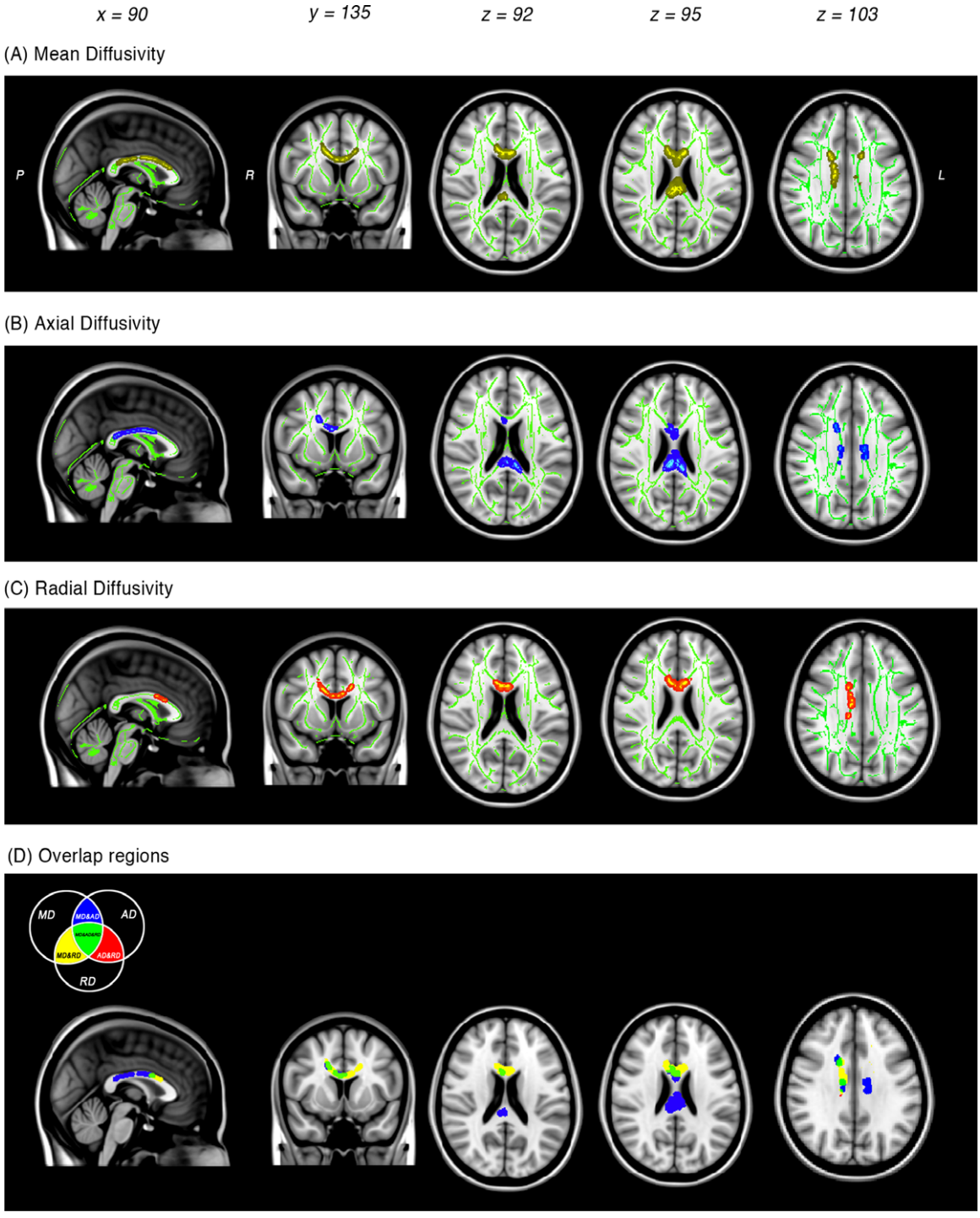

Figure 1. Brain regions with significant abnormal diffusion tensor imaging metrics. Patients with IIH compared with patients without IIH and primary headache disorder, showed significantly lower (A) mean diffusivity (MD, in yellow), (B) axial diffusivity (AD, in blue), and (C) radial diffusivity (RD, in red) ($P < 0.05$, FWE corrected). (D) Brain regions with abnormal diffusion tensor imaging (DTI) properties in patients with IIH, where the three significant metrics overlap. The regions with lower MD, AD, and RD are showed in green. The abnormal brain regions with lower MD and lower AD are colored in blue. The overlapping regions with lower AD and lower RD (in red) result to be the same of the overlapping of lower MD and lower RD (in yellow). On the left of panel D is the diagrammatic drawing with regards to the colors and the relationship of the overlap. R: right; L: left; P: posterior; FWE: family wise error rate.

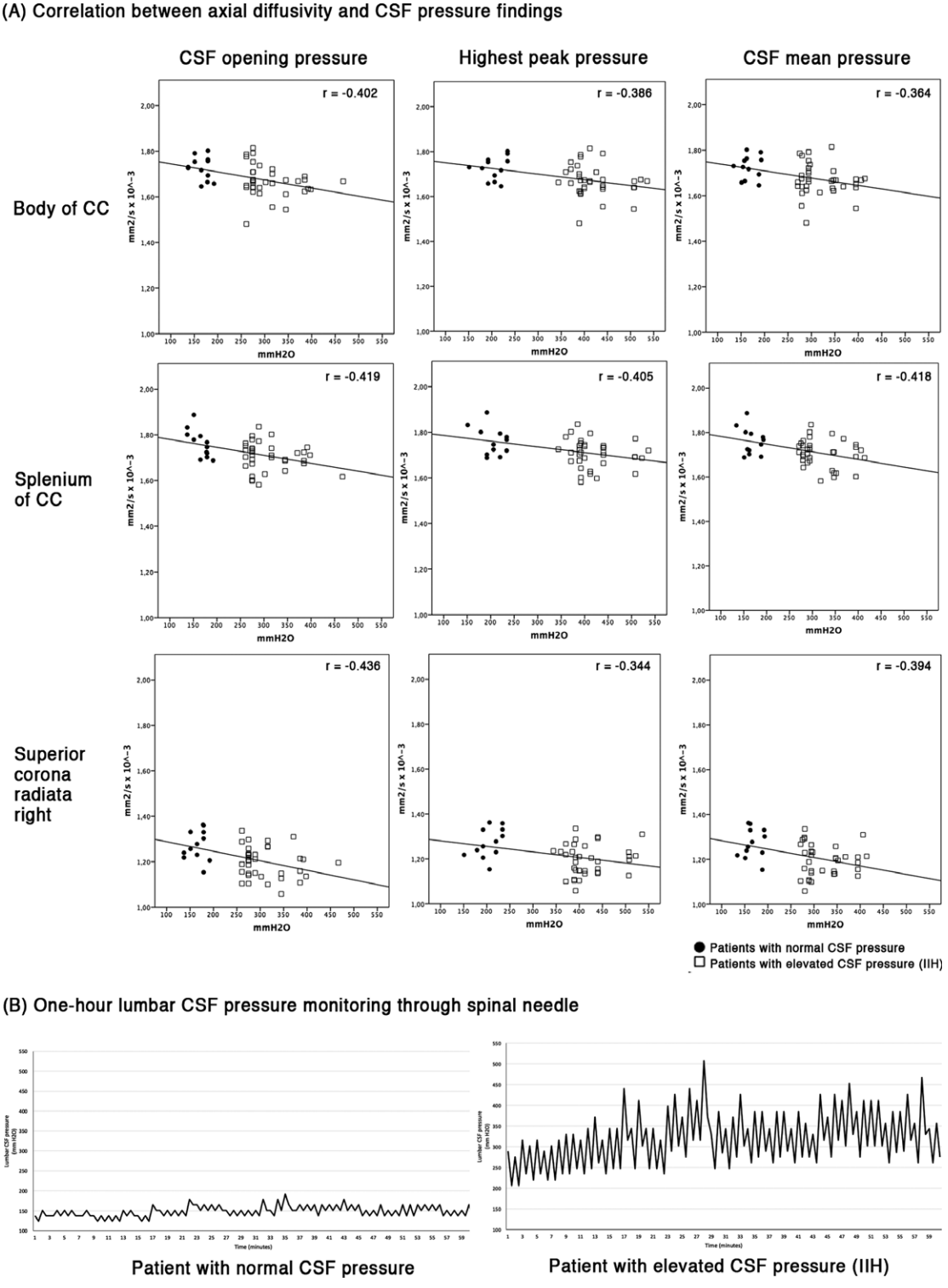

Figure 2. Regression between abnormal diffusion metrics and CSF pressure values in 37 patients with IIH and 12 patients without IIH. (A) The correlation analysis demonstrated that there were significant negative correlations between values of pressure and the average axial diffusivity (AD) in the body and splenium of corpus callosum (CC) and in the right superior corona radiata. Average AD and RD are expressed in units of $mm^2/sec \times 10^{-3}$. (B) One-hour lumbar CSF pressure monitoring through a spinal puncture needle of a patient with normal CSF pressure (on the left) and of a patient with elevated CSF pressure (on the right).

Table 4. Rating scale scores, CSF pressure findings, and DTI metrics at baseline and at follow-up in eight treated patients with idiopathic intracranial hypertension.

			Patients with IIH at the baseline	Patients with IIH at the follow-up
VAS			8.37 ± 1.18	2 ± 0.75[1]
MIDAS			23.37 ± 7.31	7.37 ± 4.24[1]
CSF pressure, mmH_2O				
Opening pressure			308.25 ± 98.97	170 ± 17.99[1]
Mean pressure			282.87 ± 57.59	164.12 ± 18.81[1]
Highest peak pressure			392.25 ± 71.34	204.37 ± 27.15[1]
WM regions	Side	Metric		
Anterior corona radiata	Right	MD	0.72 ± 0.03	0.77 ± 0.03[1]
	Left		0.70 ± 0.03	0.74 ± 0.02[1]
Superior corona radiata	Right	MD	0.67 ± 0.05	0.72 ± 0.04[1]

Data are given as mean ± SD. Average MD are expressed in units of $mm^2/s \times 10^{-3}$.
MD, mean diffusivity, CSF, Cerebrospinal fluid, DTI, Diffusion tensor imaging. WM, white matter. IIH, idiopathic intracranial hypertension, VAS, Visual Analogue Scale, MIDAS, Migraine Disability Assessment Scale.
[1]Significant at paired *t*-test $P < 0.05$.

change in fractional anisotropy. The DTI alterations were more severe in body and splenium of corpus callosum and in the right superior corona radiata, where all the metrics were simultaneously decreased. Interestingly, these three most damaged regions corresponded to the ones that were negatively correlated with the severity of CSF-pressure elevation in patients with IIH. Moreover, the same regions of patients with IIH resulted to be altered in the post hoc comparison between patients with IIH and patients with primary headache disorder, both with chronic migraine. The underlying pathologic substrates of IIH could be inferred from the diffusion indices themselves. In fact, while MD is a measure of the average molecular motion derived from AD and RD, AD may detect longitudinal changes in the movement of water molecules along the axons and RD the perpendicular diffusion modulated by myelin sheath.[14–16] The reduction in MD, AD, and RD as in our work, could indicate changes in white matter architecture consistent in a probable tissue compaction around the ventricles.[20,21] To explain this periventricular WM microstructure changes in patients with IIH, we hypothesize that high CSF pressure causes repetitive pressure pulsations producing a mechanical compression against the wall of the lateral ventricles. This mechanism leads to a periventricular tissue compaction that prevents the normal movement of the water molecules and causes the alteration of periventricular WM microstructure.

At support of this pathophysiologic mechanism, given data demonstrate a correlation between mean AD changes and the severity of the CSF-pressure elevation in patients with IIH. Indeed, previous DTI studies in hydrocephalus (HCP)[22,23] also found a relationship between altered diffusion metrics and high CSF pressure. At variance with DTI analysis findings in patients with HCP, we did not find an increase in FA in fibers lateral to ventricles and a decrease in the corpus callosum parts that lie above the ventricles.[22] Since increased FA on DTI correlated with enlargement of the ventricles in patients with HCP,[23] the absence of FA alterations could be explained by the lack of the enlargement of lateral ventricles in our patients with IIH. On other hand, the lack of significant changes in FA of patients with IIH could have another explanation. It may occur when the absolute values of AD and RD are similarly decreased, so that their ratio remains the same.[24,25]

In the current study, TBSS analysis revealed changes in diffusion metrics confined to periventricular WM in patients with IIH. By contrast, several DTI studies showed the presence of extensive DTI microstructure alterations in WM of multiple brain regions in patients with primary headache disorders.[21,26] The discrepancy between our results and the abovementioned studies may be explained by the different mechanisms causing the changes of WM microstructure. In patients with IIH the periventricular area is the anatomical region directly subjected to the compressive action of the abnormal CSF pressure pulsations in IIH. This pathogenic mechanism thus causes the periventricular WM microstructure alterations leading to the focal DTI findings in our patients with headache attributed to IIH. Whereas, the extensive WM microstructure alterations found in above mentioned studies[21,26] may be explained by the hyperexcitability of the whole brain in migraine.

There are limitations to this study, given the fact that lumbar CSF pressure monitoring lasted one hour, only eight treated patients with IIH agreed to undergo continuous CSF pressure monitoring during the follow-up. For this reason, in the longitudinal TBSS analysis we included only a small group of treated patients with IIH. Another limitation may be linked to the use of not a particularly high number of diffusion encoding directions in our DTI study. However, it should be mentioned that a recent methodological work[27] demonstrated that no significant differences were detected in FA maps with 13, 27, or 55 encoding directions. Since our acquisition protocol consisted of 27 diffusion encoding directions, the results of abovementioned study confirm the quality of our DTI measurements. A further limitation of the present study is that only 12 of 27 patients of the group without IIH underwent the LP and the 1-hour lumbar CSF pressure monitoring. Indeed, the clinical features and neuroimaging findings did not support the diagnosis of elevated intracranial pressure in the remaining 15 patients. Anyway, a supplementary analysis restricted to those patients without IIH and with CSF measurement, revealed that the differences in the diffusion metrics involved the same brain regions, compared with the group with IIH (Table S1).

The present study highlights that there is a continuous and graded relation between severity of the CSF-pressure elevation and the periventricular WM microstructure changes in patients with IIH. Importantly, our results showed that DTI alterations were partially reversible when CSF pressure normalized after medical treatment in a small group of patients with IIH. This fact suggests that DTI may be used to track disease progression or resolution, and to assess the efficacy of treatment.

Acknowledgments

We thank the patients for their participation to this study, and the radiology technicians Domenico Gullà and Federico Rocca.

Author Contributions

Dr Sarica: analyses and interpretation of the data, statistical analysis, and drafting/revising the manuscript, final approval of the version to be published. Dr Curcio: data collection, analysis and interpretation, and drafting/revising the manuscript, final approval of the version to be published. Dr Rapisarda: acquisition of data and analysis of data, drafting/revising the manuscript, final approval of the version to be published. Dr. Cerasa drafting/revising the manuscript, final approval of the version to be published. Prof Quattrone: drafting/revising the manuscript, final approval of the version to be published. Dr. Bono: study concept and design, acquisition, analysis, and interpretation of the data, drafting/revising the manuscript for important intellectual content, final approval of the version to be published.

Conflicts of Interest

Nothing to report.

References

1. Friedman DI, Liu GT, Digre KB. Revised diagnostic criteria for the pseudotumor cerebri syndrome in adults and children. Neurology 2013;81:1159–1165.
2. Giuseffi V, Wall M, Siegel PZ, Rojas PB. Symptoms and disease associations in idiopathic intracranial hypertension (pseudotumor cerebri): a case-control study. Neurology 1991;41:239–244.
3. Wall M, George D. Idiopathic intracranial hypertension. A prospective study of 50 patients. Brain 1991;114 (Pt 1A):155–180.
4. Bruce BB, Preechawat P, Newman NJ, et al. Racial differences in idiopathic intracranial hypertension. Neurology 2008;70:861–867.
5. Bono F, Messina D, Giliberto C, et al. Bilateral transverse sinus stenosis predicts IIH without papilledema in patients with migraine. Neurology 2006;67:419–423.
6. Bono F, Messina D, Giliberto C, et al. Bilateral transverse sinus stenosis and idiopathic intracranial hypertension without papilledema in chronic tension-type headache. J Neurol 2008;255:807–812.
7. Messina D, Bono F, Fera F, et al. Empty sella and bilateral transverse sinus stenosis predict raised intracranial pressure in the absence of papilloedema: a preliminary study. J Neurol 2006;253:674–676.
8. Agid R, Farb RI, Willinsky RA, et al. Idiopathic intracranial hypertension: the validity of cross-sectional neuroimaging signs. Neuroradiology 2006;48:521–527.
9. Bidot S, Saindane AM, Peragallo JH, et al. Brain imaging in idiopathic intracranial hypertension. J Neuroophthalmol 2015;35:400–411.
10. Farb RI, Vanek I, Scott JN, et al. Idiopathic intracranial hypertension: the prevalence and morphology of sinovenous stenosis. Neurology 2003;60:1418–1424.
11. Bono F, Lupo MR, Lavano A, et al. Cerebral MR venography of transverse sinuses in subjects with normal CSF pressure. Neurology 2003;61:1267–1270.
12. Alperin N, Oliu CJ, Bagci AM, et al. Low-dose acetazolamide reverses periventricular white matter hyperintensities in iNPH. Neurology 2014;82:1347–1351.
13. Bono F, Salvino D, Tallarico T, et al. Abnormal pressure waves in headache sufferers with bilateral transverse sinus stenosis. Cephalalgia 2010;30:1419–1425.

14. Pierpaoli C, Basser PJ. Toward a quantitative assessment of diffusion anisotropy. Magn Reson Med 1996;1996:893–906.
15. Jones DK, Leemans A. Diffusion tensor imaging. Methods Mol Biol 2011;2011:127–144.
16. Mori S, Zhang J. Principles of diffusion tensor imaging and its applications to basic neuroscience research. Neuron 2006;2006:527–539.
17. Headache Classification Committee of the International Headache Society. The International Classification of Headache Disorders, 3rd edition (ICHD-3). Cephalalgia 2018.
18. Fera F, Bono F, Messina D, et al. Comparison of different MR venography techniques for detecting transverse sinus stenosis in idiopathic intracranial hypertension. J Neurol 2005;252:1021–1025.
19. Sarica A, Cerasa A, Valentino P, et al. The corticospinal tract profile in amyotrophic lateral sclerosis. Hum Brain Mapp 2017;38:727–739.
20. Smith SM, Jenkinson M, Johansen-Berg H, et al. Tract-based spatial statistics: voxelwise analysis of multi-subject diffusion data. NeuroImage 2006;31: 1487–1505.
21. Benedetti F, Yeh PH, Bellani M, et al. Disruption of white matter integrity in bipolar depression as a possible structural marker of illness. Biol Psychiatry 2011;69:309–317.
22. Messina R, Rocca MA, Colombo B, et al. White matter microstructure abnormalities in pediatric migraine patients. Cephalalgia 2015;35:1278–1286.
23. Assaf Y, Ben-Sira L, Constantini S, et al. Diffusion tensor imaging in hydrocephalus: initial experience. AJNR Am J Neuroradiol 2006;27:1717–1724.
24. Daouk J, Chaarani B, Zmudka J, et al. Relationship between cerebrospinal fluid flow, ventricles morphology, and DTI properties in internal capsules: differences between Alzheimer's disease and normal-pressure hydrocephalus. Acta Radiol 2014;55:992–999.
25. Maller JJ, Thomson RH, Pannek K, et al. The (Eigen)value of diffusion tensor imaging to investigate depression after traumatic brain injury. Hum Brain Mapp 2014;35:227–237.
26. Yu D, Yuan K, Qin W, et al. Axonal loss of white matter in migraine without aura: a tract-based spatial statistics study. Cephalalgia 2013;33:34–42.
27. Yoshikawa T, Aoki S, Abe O, et al. Diffusion tensor imaging of the brain: effects of distortion correction with correspondence to numbers of encoding directions. Radiat Med 2008;26:481–487.

Supporting Information

Additional supporting information may be found online in the Supporting Information section at the end of the article.

Table S1. Diffusion tensor imaging metrics of white matter regions significantly different between patients with (35) and without (12) increased intracranial pressure and with CSF measurement.

